



Depercolation threshold of porosity in model cement: approach by morphological evolution during hydration

J. Hu *, P. Stroeven

Faculty of Civil Engineering and Geosciences, Delft University of Technology, Stevinweg 1, 2628 CN Delft, The Netherlands

Received 15 April 2003; accepted 13 February 2004

Abstract

The depercolation threshold of porosity is an important parameter to assess the permeability of cement-based materials. The depercolation threshold is usually defined as the porosity whereby the volume fraction of connected pores in the cement paste decreases to zero. In this paper, the depercolation threshold is defined and determined with respect to the morphological development of pore space during hydration. The morphology of solid phase and pore structure is studied on model cement simulated by the SPACE system, using stereological theory. The influences of particle size distribution and water to cement ratio (w/c) on the depercolation threshold of porosity are discussed. It is found that particle size distribution of cement has significant influence on the depercolation threshold of porosity. The depercolation threshold is higher for finer cement system. However, the influence of w/c on the depercolation threshold of porosity is negligible. For a model cement of moderate fineness, depercolation is not possible at a relatively high w/c (say, 0.6), because the porosity of cement paste remains above the depercolation threshold even at complete hydration.

© 2004 Elsevier Ltd. All rights reserved.

Keywords: Depercolation threshold of porosity; Morphological evolution; Particle size distribution; SPACE simulation; Water to cement ratio

1. Introduction

The durability of a cementitious material largely depends on the possibility of penetration of hazardous ions into the porous material with water as medium. The water permeability of the cementitious material is very crucial to its durability. The permeability of cement-based materials can be experimentally measured, but the accuracy of the results of these time-consuming experiments relies on care bestowed on sample preparation and on experimental conditions. As a promising alternative, computer simulation of packing and hydration of a model cement offers insight into the depercolation process of pore space, which is associated with the permeability of cement paste. Various research studies have been carried out, based on different modeling concepts, which emphasized the depercolation threshold of capillary porosity, denoted as p_c as a function of technical parameters, among which particle size distribution

(PSD) and water to cement ratio (w/c) are of most importance. Bentz and coworkers [1,2] made a preliminary investigation on the depercolation threshold of porosity for two cement systems of different finenesses. A depercolation threshold of porosity of 18% was found for a coarse cement with median grain diameter of about 22 μm , while the threshold value was 22% for a relatively fine cement with median grain diameter of about 4 μm . However, Elam et al. [3] found the depercolation threshold of a sphere-based numerical model cement to be around a few percent porosity. Also based on a model cement composed of spherical particles, Ye et al. [4] reported that the depercolation of capillary pores cannot be realized because the pore structure remains highly interconnected even at the ultimate hydration stage. The obvious divergence between various research outcomes can at least be attributed partially to the characteristics of simulation models and to the digital resolution. The afore-mentioned conclusions are based on the definition of p_c as the porosity whereby the fraction of connected pores decreases to zero. In the present study, the depercolation of pore space is studied in view of the morphological

* Corresponding author. Tel.: +31-15-278-2307; fax: +31-15-278-8162.

E-mail address: j.hu@citg.tudelft.nl (J. Hu).

evolution of pore phase during hydration, employing SPACE simulation. SPACE (Software Package for Assessment of Compositional Evolution) [5] was developed for computer simulation of cement packing and hydration. It does not rely on a random generation process of particle positions. As a result, it has been demonstrated to offer relatively realistic simulation of the packing structure of spherical cement particles with various particle size distributions [6]. Some stereological estimation is integrated into the package and has been used to evaluate the extent of the Interfacial Transition Zone (ITZ). In this study, the morphology of solid phase and pore structure is determined on the basis of stereological estimation incorporated in SPACE. The influences of particle size distribution and w/c on the depercolation threshold of capillary porosity are studied.

2. Theoretical background

2.1. SPACE simulation of model cement and hydration

The simulation approach is based on a non-continuous representation of the internal material structure. Cement particles with predefined size distribution (Rosin–Rammler distribution in this study, which is proven to be a satisfactory approximation of the size distribution of actual unhydrated cement particles) are generated within the boundaries of a cubical container. Next, physical properties can be assigned to each element to realize ‘dynamic mixing’ until a desired volume fraction of cement particles (corresponding to a certain w/c ratio) is reached. The model cement is then subjected to hydration according to the kinetics of cement hydration. Detailed description of the SPACE system is available in [5].

2.2. Morphology of solid phase and pore space in model cement

The model cement is considered to be composed of solid phase and pore space. Initially, the pore space is entirely connected. The solid phase consists of unhydrated cement and hydration products. The volume fraction of solid phase is continuously increasing as a result of hydration. The solid phase starts from individual spherical particles that gradually get interconnected to form a microstructure network. The fractional connectivity of pore phase, or fraction of connected porosity, decreases monotonically at a given w/c as hydration proceeds, and parts of the capillary pore space become isolated. A point is reached for lower w/c where pore connectivity drops rapidly at continuing hydration, ultimately leading to discontinuity in the capillary pore structure. The value of porosity p and

degree of hydration α at which this occurs are denoted by p_c (depercolation threshold of capillary porosity) and α_c (the critical degree of hydration for depercolation), respectively.

The solid phase is complementary to pore space in model cement. Therefore, the morphological and geometrical properties of solid phase are indirect representations of the morphology of pore structure. Size and the spatial distribution of solid phase can be characterized by the mean intercept length of solid clusters \bar{L}_3 and the mean free distance between solid clusters λ , respectively. These operators are available in the SPACE system. The definition of these stereological descriptors—though self-explanatory—can be found in [7].

One important stereological parameter to characterize the microstructure of hydrated cement is the surface area of solid phase per unit of test volume (the container), $(S_V)_{\text{test}}$. This parameter can be directly measured with tessellation on the surface of solid phase and recorded as a function of hydration time. It can also be calculated from perimeter length of pore features (or solid clusters) per unit of test area L_A (that can be determined by section image analysis) by way of the relationship $(S_V)_{\text{test}} = 4L_A/\pi$ [7]. The volume fraction of solid phase, V_V and porosity, $p = 1 - V_V$, can be determined easily at a certain hydration time. For hydrated cement, the following parameters can be obtained:

$$\bar{L}_3 = 4 \frac{V_V}{(S_V)_{\text{test}}} \quad (1)$$

$$\lambda = 4 \frac{1 - V_V}{(S_V)_{\text{test}}} \quad (2)$$

It can be seen from Eqs. (1) and (2) that the mean free distance between solid clusters (λ) equals the mean intercept length of pore space. Therefore, λ is a direct representation of the size of pore space. The decreasing function of λ versus hydration time can be used to determine the depercolation threshold p_c . A comparison between model cements with various w/c ratios and finenesses allows characterizing the influences of these important technical parameters on the depercolation threshold.

3. Materials design and modeling

Three model cements of different finenesses were generated in this study [8]. The Blaine specific surface areas were 167 m²/kg (cement C167), 342 m²/kg (cement C342) and 605 m²/kg (cement C605), corresponding to coarse, ordinary and fine cement, respectively. The size of the particles of the model cements is approached using the Rosin–Rammler particle size distribution function, $G(d) = 1 - \exp(-bd^n)$, in which n and b are constants [9]. The particle size distribution (PSD) curves

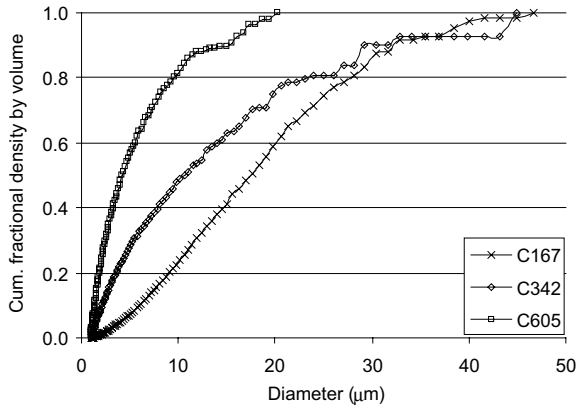


Fig. 1. Cumulative particle size distribution curves for model cements C167, C342 and C605. The mixtures were generated by the SPACE system.

are shown in Fig. 1. The mixtures were compacted to fractional volume densities of 0.51, 0.44, 0.39, and 0.35, corresponding to w/c of 0.3, 0.4, 0.5 and 0.6, respectively. The mixtures were hydrated for up to 100,000 h. The morphological evolution of solid phase and pore space were measured and recorded as hydration proceeded.

4. Results and discussion

4.1. Depercolation threshold of capillary porosity

The evolution of λ during 10,000 h of hydration is shown in Fig. 2 for cement C342 with various w/c. Changes after 10,000 h are only minor. A decreasing function of λ versus hydration time could be expected. The starting point of the curve is the mean free distance

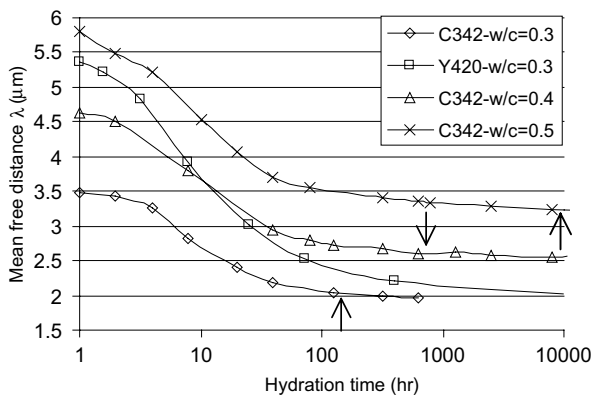


Fig. 2. Profile of morphological evolution of pore space in C342 (SPACE simulation, size range 1–45 μm), at w/c ranging between 0.3 and 0.5 (the depercolation threshold indicated with arrow); the change for model cement Y420 (HYMOSTRUC simulation, $S_G = 420 \text{ m}^2/\text{kg}$, size range 2–45 μm , see [4] for the PSD curve) is also presented for comparison.

Table 1
Depercolation parameters of capillary porosity for paste C342

w/c	p_c (%)	t_c (h)	α_c (–)	λ_0 (μm)	λ_{end} ($t = t_c$)
0.3	21.1	126	0.42	3.5	2.0
0.4	21.3	631	0.57	4.6	2.6
0.5	23.4	7943	0.76	5.8	3.2

in the initial packing structure, λ_0 . It should be noted that the mean free distance drops rapidly in the first day (or so), then gradually decreases to a certain value λ_{end} that only marginally diminishes at further increase of hydration time. The critical point where the plateau is reached (the first point approaching λ_{end} within $\pm 3\%$ relative variation from the value of λ_{end}) corresponds to a porosity of 21% for w/c = 0.3 paste. Since λ is a direct observation of the pore size, this point can be related to the depercolation threshold of capillary porosity. The parameters at depercolation for cement of various w/c are presented in Table 1, and will be discussed in what follows.

The traditional way [1–4] to determine p_c by computer simulation is calculating the volume fraction of connected pores and define the threshold as the porosity when the connected porosity decreases to zero. Bentz et al. from NIST [2] reported a threshold between 18% and 22% for ordinary cement with Rosin–Rammler distribution. This is in agreement with the result in this study. In a pixel-based model such as the NIST simulation, various cement components are simulated by different sets of pixels without any constraint on shape of these components. In contrast, SPACE and HYMOSTRUC [9] (the basis of Ye’s [4] simulation) start from packed spherical cement particles and are based on the same hydration kinetics. One major difference between the two models is that HYMOSTRUC adopts a ‘random packing’ concept, whereas SPACE employs a ‘dynamic mixing’ algorithm to realize the densification of the cement particle system [5]. Ye et al. [4] found that the pore structure remains highly interconnected even when the cement (w/c varying between 0.3 and 0.6) reaches the ultimate hydration stage (porosity about 3%). As a consequence, no depercolation was observed in his study. He attributed this finding to the high digital resolution (0.25 $\mu\text{m}/\text{pixel}$, hence tiny capillary pore pathways can be detected) and the assumption of spherical cement particles. In the NIST model, the depercolation threshold of the capillary porosity changed from 24% to 18% and 12% in a cement paste with w/c of 0.3 when the digital resolution shifted from 1 to 0.5 and 0.25 $\mu\text{m}/\text{pixel}$, respectively [2]. So, even at the same resolution of 0.25 $\mu\text{m}/\text{pixel}$, the NIST system and the HYMOSTRUC model revealed striking differences in depercolation porosity. The morphological evolution of cement Y420 with w/c of 0.3 (simulated by HYMOSTRUC, with a specific surface area of 420 m^2/kg) is also plotted in Fig. 2 as comparison to that of

C342. The value of λ_0 is 5.7 μm for Y420, while the value for C342 ($w/c=0.3$) is 3.5 μm , although Y420 is finer than C342. This phenomenon can be partially explained by the big interval of PSD for Y420, i.e., 1 μm , while the PSD of C342 is a more continuous one with size interval of 0.02 μm .

4.2. Influence of technical parameters

In the initial study of Bentz and Garboczi [10], based on a simple model of C_3S hydration only, a depercolation threshold of about 18% was identified for capillary porosity. Using the most recent version of the NIST microstructure model, Bentz et al. [1] studied the depercolation for two cement PSDs (with median grain size of $\langle 5 \mu\text{m} \rangle$ and $\langle 30 \mu\text{m} \rangle$, corresponding to a fine cement and a coarse one, respectively; see [1] for details of PSD) at three different w/c (0.246, 0.3 and 0.5). The depercolation threshold p_c was determined as the porosity whereby fractional connectivity declined to zero. It was found that the cement PSD had a significant effect on the capillary porosity at which depercolation occurs. Compared to the effects of PSD, those of w/c ratio were of minor importance. In general, the depercolation threshold for the $\langle 30 \mu\text{m} \rangle$ system was about 18%, while that for the $\langle 5 \mu\text{m} \rangle$ system was about 22%.

4.2.1. Influence of w/c

Fig. 2 clearly reveals the curves of mean free distance versus hydration time to have similar shape for various w/c . For a higher w/c , the mean free distance is larger at equivalent hydration time because cement with higher w/c starts from a less densely packed particle system. The time when depercolation occurs t_c as well as the critical hydration degree α_c , increase with w/c , as demonstrated by the data presented in Table 1. It is interesting to note that the value of p_c is similar for cements with various w/c (about 21% for C342). This indicates that the effect of water cement ratio on depercolation threshold is negligible, which is in agreement with the observations in [1,2]. To give a better insight into the influence of w/c ratio on depercolation threshold, the

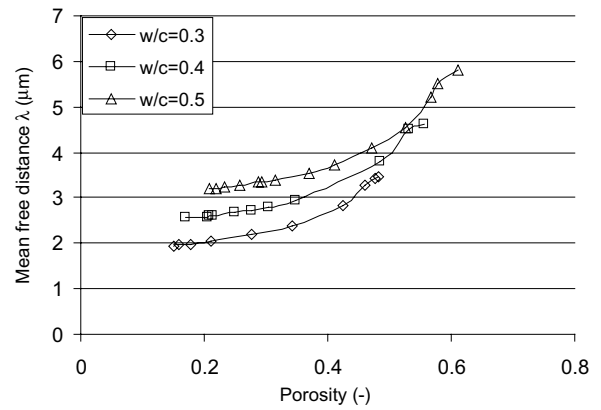


Fig. 3. Influence of water to cement ratio on the depercolation threshold of capillary porosity.

mean free distance is plotted against porosity in Fig. 3. The curves for various w/c slightly deviate from each other, suggesting a degree of self-similarity in the hydration process.

In case of cement with w/c of 0.6, although the pore space also becomes less connected as hydration progresses, the depercolation threshold cannot be reached because the high initial porosity prevents closing off the water-filled pore space with hydration products. In this case, it is not possible for the cement to hydrate sufficiently to achieve depercolation of the capillary porosity. Bentz et al. [1] reported that the depercolation curve (connected fraction versus capillary porosity) for w/c of 0.6 approaches asymptotically those of the lower w/c ratios. The cement with w/c of 0.6 had a final porosity of 26% at the ultimate hydration stage. According to Powers' model, a cement with w/c of 0.6 has an estimated final porosity of 25%. This accounts for the observation that the cement of $w/c=0.6$ cannot depercolate because the porosity at complete hydration is still higher than the depercolation threshold.

4.2.2. Influence of the particle size distribution

The PSD and depercolation parameters for the three model cements C167, C342 and C605, at w/c of 0.3 are given in Table 2 and Fig. 4. For coarser cement, the

Table 2
PSD and morphological parameters of the model cements ($w/c=0.3$)

Cement code		C167	C342	C605
PSD parameters	Size range (μm)	1–47	1–45	1–20
	n	1.836	1.083	1.193
	b	0.004	0.054	0.111
	Median diameter (μm)	17.6	10.6	4.2
Morphological parameters	λ_0 ($t=0$, μm)	6.7	3.4	2.0
	λ_{end} ($t=t_c$, μm)	2.7	2.0	1.2
Depercolation	p_c (%)	7.9	21.1	31.8
	t_c (h)	794	126	40
	α_c (-)	0.52	0.42	0.33

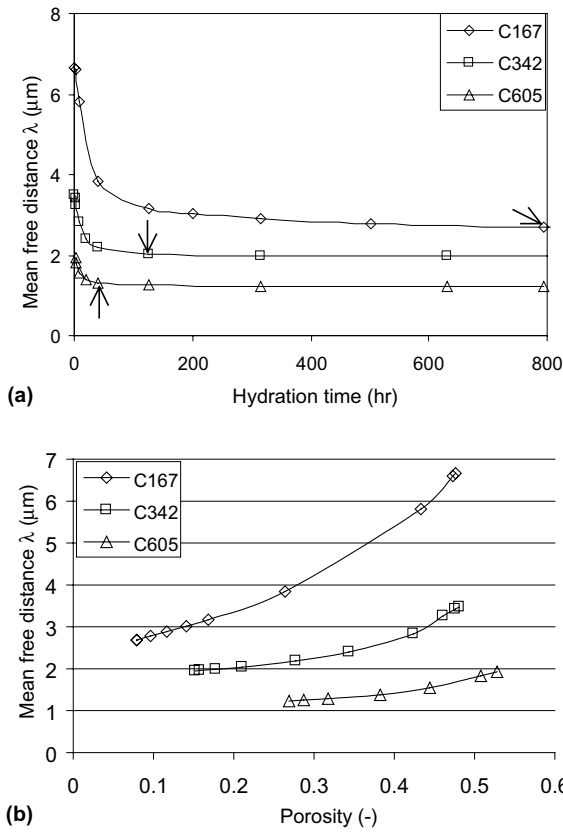


Fig. 4. Influence of PSD on depercolation threshold of pore space: (a) evolution of mean free distance versus hydration time (the depercolation threshold indicated with arrow); (b) evolution of mean free distance versus porosity.

average interparticle spacing is larger, so that more extensive hydration and longer hydration time is required to close off the capillary porosity.

The finer cement hydrates far more rapidly, independent of w/c , hence, it reaches the depercolation threshold within a shorter period of time. Therefore, when evaluating the depercolation of cement paste of widely varying PSDs, one must be careful to distinguish hydration kinetics effects from microstructural effects. For this purpose, the morphological evolution for the three cements is plotted in Fig. 4b against a microstructural parameter, total capillary porosity, instead of plotting it against hydration time as in Fig. 4a. Eventually, for lower w/c such as 0.3, the coarser cement's hydration will catch up with that of the finer one, and the final mean free distance λ_{end} will be similar for the three model cements.

5. Implication for material performance

5.1. Curing time

Depercolation has been discussed by Bentz and Haecker [11] in terms of the 'curability' of the concrete.

Once the capillary porosity depercolates in a cement paste, the imbibition of water to replace that lost due to chemical shrinkage during hydration slows down significantly, as the transport controlling mechanism shifts from the capillary pores to the much smaller gel pores. Thus, the longer it takes for the capillary porosity to disconnect, the longer one has to continue to add water to the interior of the concrete. This implies an increased 'curability' for the coarser cement systems.

5.2. Diffusivity

Although diffusivity is not directly dependent on pore size, it is directly proportional to pore connectivity, which is higher in a paste with larger pores, such as the coarse cement C167. On the other hand, diffusivity is inversely proportional to pore tortuosity, which will be decreased in systems with larger pores. For coarser cement, the pore size (represented by λ in Fig. 4) is larger than for finer cement at equivalent hydration time. As a result of higher pore connectivity and lower pore tortuosity in the coarser cement, its diffusivity is expected to be higher than in the case of a finer cement.

Bentz et al. [1] studied the diffusivity of model cements for two PSD ($\langle 5 \mu\text{m} \rangle$ and $\langle 30 \mu\text{m} \rangle$) systems. For capillary porosities above the depercolation threshold, the relative diffusivities of the coarser cements (the diffusion coefficient of an ion in the concrete relative to its value in free water) are about twice those of a finer cement with the same porosity. It is found that after the capillary porosity depercolates, the relative diffusivities of the two different systems are much more similar. This is in agreement with the above-mentioned theoretical analysis.

5.3. Permeability

The permeability of cement paste is closely correlated to pore size and pore connectivity. According to the Carmen–Kozeny model, the permeability k of cement paste can be predicted on the basis of the geometrical properties of the pore space by:

$$k = \frac{p(V_{\text{pore}}/S_{\text{pore}})^2}{2\beta} \quad (3)$$

where p is the porosity, V_{pore} and S_{pore} are the volume and the internal surface area of pore space, and β is the tortuosity of the transport route in the cement. Permeability is proportional to the second power of $V_{\text{pore}}/S_{\text{pore}} = \lambda/4$. Eq. (2) allows calculating λ . Stroeven [12] demonstrated by a stereological approach that the tortuosity of transport paths in spherical aggregate concrete does not depend on the size distribution of the aggregate particles. Hence, details of the sieve curve will not exert influence on transport phenomena of concrete.

Tortuosity of the transport route can be estimated only from a single morphological parameter, i.e. volume fraction of aggregates, $\beta = 1 + V_V/2$. Assuming this to hold also for transport through the paste, Eq. (3) can be transformed into:

$$k = \frac{(1 - V_V)\lambda^2}{32 + 16V_V} \quad (4)$$

The estimated permeability for cement C342 with various w/c is shown in Fig. 5 and the results for model cements with different finesses are plotted in Fig. 6. The discrete points are experimental permeability results taken from the literature for a cement with moderate fineness [13]. The mean free distance has a pronounced influence on transport properties of cement paste. It is clear that the permeability of C605 is much lower than that of C167 at the early hydration stages, and eventually reaches similar values of about $1 \times 10^{-17} \text{ m}^2$ at low porosity. This is in agreement with the findings of Bentz et al. [1,2].

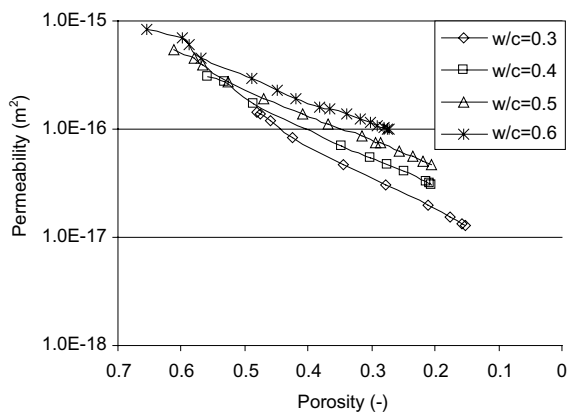


Fig. 5. Predicted permeability of cement paste C342 with various w/c.

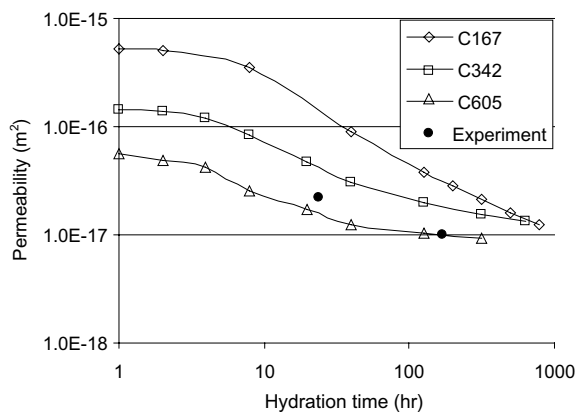


Fig. 6. Influence of cement fineness on the permeability of cement paste.

When the predicted permeability is plotted against degree of hydration of the model cement, the results are found consistent with the experimental data for cement paste available in [14]. Powers et al. [14] defined capillary pore discontinuity as the point at which the measured fluid permeability, as a function of hydration degree α , showed a marked change in slope.

6. Conclusion

The SPACE system is able to properly simulate in its fresh state the packing of cement particles with Rosin–Rammler size distribution. Additionally, hydration process of the cement can be implemented. The parameter $(S_V)_{\text{test}}$ of the solid phase can be estimated by the SPACE system during the hydration process. The mean free distance between solid clusters can be determined by a stereological test and is a direct measure for pore size. The depercolation threshold of capillary porosity can be estimated within the framework of the morphological evolution of pore structure as hydration proceeds. The particle size distribution of cement has a significant effect on the depercolation threshold, while the effect of water cement ratio is only of minor significance. The finer cement has a higher depercolation threshold of capillary porosity because of two factors: (i) the interparticle spacing is smaller, therefore it is easier for finer cement to close off pore space; (ii) at a given water to cement ratio, the finer cement hydrates more rapidly, hence it takes less time to achieve depercolation of capillary porosity.

References

- [1] Bentz DP, Garboczi EJ, Haecker CJ, Jensen OM. Effects of cement particle size distribution on performance properties of portland cement-based materials. *Cem Concr Res* 1999;29:1663–71.
- [2] Garboczi EJ, Bentz DP. The effect of statistical fluctuation, finite size error, and digital resolution on the phase percolation and transport properties of the NIST cement hydration model. *Cem Concr Res* 2001;31:1501–14.
- [3] Elam WT, Kerstein AR, Rher JJ. Critical properties of the void percolation problem for spheres. *Phys Rev Lett* 1984;52:1516–9.
- [4] Ye G, van Breugel K, Fraaij ALA. Three-dimensional microstructure analysis of numerically simulated cementitious materials. *Cem Concr Res* 2003;33:215–22.
- [5] Stroeven M. Discrete numerical modeling of composite materials. Ph.D. Thesis, Delft University of Technology, Delft, 1999, p. 224.
- [6] Stroeven P, Stroeven M. Assessment of packing characteristics by computer simulation. *Cem Concr Res* 1999;29:1201–6.
- [7] Underwood EE. Quantitative stereology. Reading (Ma): Addison-Wesley Publishing Company; 1970. pp. 274.
- [8] Chen H. Computer simulation by SPACE of the microstructure of the ITZ between aggregate and cement paste. Report CM 2002-001. Delft University of Technology, Delft, 2002, p. 25.

- [9] van Breugel K. Simulation of hydration and formation of structure in hardening cement-based materials. Ph.D. Thesis. Delft, Delft University of Technology, 1991, p. 295.
- [10] Bentz DP, Garboczi EJ. Percolation of phases in a three-dimensional cement paste microstructure model. *Cem Concr Res* 1991;21:325–44.
- [11] Bentz DP, Haecker CJ. An argument for using coarse cements in high performance concrete. *Cem Concr Res* 1999;29:615–8.
- [12] Stoeven P. A stereological approach to roughness of fracture surfaces and tortuosity of transport paths in concrete. *Cem Concr Compos* 2000;22:331–41.
- [13] Banthia N, Mindess S. Permeability measurement on cement paste. In: Roberts LR, Skalny JP, editors. *Proceedings of Material Research Society Symposium 137*, Boston, 1989. p. 173–9.
- [14] Powers TC, Copeland LE, Mann H. Capillary continuity or discontinuity in cement pastes. *PCA Bull* 1959;110:3–12.